Supplementary Information for

Multi-block Polyesters Demonstrating High Elasticity and Shape Memory Effects

Yunqing Zhu[1], Madalyn R. Radlauer[2], Deborah K. Schneiderman[2], Milo S.P. Shaffer,[3] Marc A. Hillmyer[2]*, Charlotte K. Williams[1]*

1. Chemistry Research Laboratory, Department of Chemistry, University of Oxford, Oxford OX1 3TA, UK.

2. Department of Chemistry, University of Minnesota, Minneapolis, USA.

3. Department of Chemistry, Imperial College London, London SW7 2AZ, UK.

Content

***Materials*:** All solvents and reagents were obtained from commercial sources (Aldrich and Fisher) and used as received unless stated otherwise. ε-Decalactone (ε-DL) was dried over calcium hydride for three days, purified by vacuum transfer and was stored under nitrogen. Cyclohexene oxide (CHO) was dried over calcium hydride, fractionally distilled (twice) and was stored under an inert atmosphere. Phthalic anhydride (PA) was purified by dissolution in benzene, filtering the insoluble impurity (phthalic acid as established using ^{1}H NMR spectroscopy), crystallization from $CHCl_3$ and sublimation. MDI was purified by dissolution in hexane, filtering the insoluble impurity and removal of all the solvent in vacuo. Toluene were distilled from sodium and stored under nitrogen. The zinc catalyst **1** ($[LZn_2(Ph)_2]$ (Fig. S1) was prepared and characterized according to published methods.[1,2]

***Characterization*: *SEC*.** The polyesters were dissolved in SEC grade THF and filtered through a 0.2 μm syringe filter prior to analysis. SEC, Shimadzu LC-20AD, was used to characterize the molecular weights and polydispersities equipped with multi-detectors Refractive Index (RI) and two Mixed Bed PSS SDV linear S columns. THF was used as the eluent, at a flow rate of 1.0 mL/min at 30 °C.

***NMR*.** ^{1}H, ^{13}C nuclear magnetic resonance spectra were recorded using a Bruker AV 400 MHz spectrometer at 303 K, in $CDCl_3$, unless mentioned otherwise.

Thermal Analyses: The thermal properties were measured using DSC Q2000 (TA Instruments, UK). A sealed empty crucible was used as a reference, and the DSC was calibrated using indium. Samples were heated from room temperature to the predetermined temperature, at a rate of 10 °C min^{-1}, under helium flow, and were kept at that temperature for 2 min to erase the thermal history. Subsequently, the samples were cooled to another predetermined temperature, at a rate of 10 °C min^{-1}, and kept at that temperature for further 2 min, followed by a heating procedure from the predetermined lower temperature to the higher temperature, at a rate of 10 °C min^{-1}. Each sample was run for three heating/cooling cycles. The glass transition temperatures (T_g) reported are taken from the third cycle.

Tensile Tests. Solvent-cast polyester sheets were prepared by pouring DCM solutions of the polymer into a Teflon mold. The solvent was slowly evaporated, in the fume hood, at room temperature for 2 months. ^{1}H NMR spectroscopy was used to check for any solvent residues. After 2 months, the DCM peak could no longer be observed, indicating the polyester sheets are sufficiently dry for mechanical tests. Dumbbell-shaped sample bars were then cut from the polyester sheet (35 mm in length, 2.1 mm in gauge width as described in the standard, ISO 527) using a Zwick Punch (Zwick D-7900, Ulm-Einsingen Type 7102, Werk-Nr. 85688) with cutting blades. Approximately 6 months after solvent-casting, the mechanical properties including strength, elongation and Young's modulus were measured. The measurements were conducted at ambient temperature and humidity (22.0 °C and 16 %) on a Shimadzu AGS-X 500N Tensile Stress Tester instrument, at 10 mm/min extension rate, using the ISO-527 standard. The results were analyzed using TRAPEZIUMX V1.4.0 software. All values are reported as the average of three samples with confidence limits.

Dynamic Mechanical Thermal Analysis (DMTA). DMTA was performed using an RSA (RSA G2, TA instrument) in tension mode. The sample bars used for DMTA have the same dimensions as the bars used in tensile tests. The dynamic moduli were measured as a function of temperature, at a frequency of 1 Hz and a strain of 1%. Samples were heated from –50 °C to 100 °C at a heating rate of 3 °C/min. Fully stretched sample of MPBE-59 was used for the DMTA characterization with no pre-load applied (Figure S14).

Microtoming and TEM. Samples were trimmed by hand to reveal a stub with a superficial area of 250×250 μm^2, then stained with ruthenium tetroxide (RuO_4) vapour for 4 hours, to enhance contrast between microphases. RuO_4 selectively stains the aromatic PCHPE domains, resulting in the PCHPE domains appearing darker than the PDL domains during imaging. Furthermore, the RuO_4 vapor also hardens the PCHPE domain, allowing for room-temperature microtoming. After vapour staining, the samples were microtomed, at room temperature, and cut speeds of 2 to 4 mm/s, using a Leica EM UC6 ultramicrotome and a MicroStar diamond knife. This unconventional procedure permitted the blends to be readily and rapidly microtomed to give sections approximately 80 nm thick. These sections were

then collected on a tabbed copper grid (PELCO, 300 mesh), and imaged using a FEI Tecnai G2 Spirit BioTWIN transmission electron microscope operating at a 120 kV accelerating voltage.

1D X-ray scattering characterization. These analyses were performed at the Advanced Photon Source (APS) at Argonne National Laboratory at the DuPont-Northewstern Dow Collaborative Access Team (DND-CAT) Synchrotron Research Center located at Sector 5 of the APS. For these experiments the energy was 16.4000 keV, and scattering intensities were monitored using a CCD area detector at a sample to detector distance of 850 cm. All experiments were conducted at ambient temperature.

2D X-ray scattering characterization. These characterizations were performed at the University of Warwick. All characterizations were conducted at ambient temperature. Measurements were made on a Xenocs Xeuss 2.0 equipped with both Cu K_α and Mo K_α microfocus sources and a Pilatus 300k detector for SAXS measurements. In addition to this there is a separate Pilatus 100k detector setup to measure between 20 and 45° in 2θ. The q range of the data was calibrated using a silver behenate standard material. Initially the SAXS detector was positioned to give a sample to detector distance of 2.495 m.

Typical procedure for switchable catalysis to prepare triblock copolyesters[1]

The zinc complex **1** ([$LZn_2(Ph)_2$] 10.0 mg, 1.25×10^{-2} mmol), phthalic anhydride (186.0 mg, 1.26 mmol), ε-DL (325.0 μL, 1.88 mmol) and a stock solution of CHD (116.0 μL; 24.0 $mg \cdot mL^{-1}$ in CHO) were dissolved in CHO (884.0 μL, 8.91 mmol), under N_2, in a screw-cap vial charged with a stir bar. The mixture was then heated to 100 °C and left to react, under an inert atmosphere, for 4.0 h. The relative molar ratio of [**1**]/[CHD]/[CHO]/[PA]/[ε-DL] was 1/2/800/100/100. The polymerization was terminated by cooling it to ambient temperature. A crude polymer sample was isolated by removal of the excess volatiles (CHO) and this material was used for NMR spectroscopy and SEC analysis. The bulk sample was further purified by precipitation of the reaction solution (containing excess epoxide) using cold MeOH. The purified sample was used for DSC and subsequent characterizations.

Typical procedure for multi-block polyester synthesis

Typically, the triblock copolymer (PDL-*b*-PCHPE-*b*-PDL, #1 in Table 1, 2.5 g, 7.22×10^{-2} mmol), methylene diphenyl diisocyanate (MDI, 19.9 mg, 7.95×10^{-2} mmol) and $Sn(Oct)_2$ were dissolved in dry toluene (4.0 mL), under N_2, in a screw-cap vial charged with a stir bar. The mixture was then heated to 60 °C and left to react, under an inert atmosphere, for 2.0 h. The chain extension reaction was terminated by cooling it to ambient temperature. The crude multi-block polymer was isolated by precipitation from the reaction solution using MeOH.

Determination of volume fractions. The density of PDL was taken from literature.[3] As the PDL block length in this work (ca. 4.0 – 12.0 $kgmol^{-1}$) is in the same region as the ones described in literature (ca. 4.8 – 9.9 $kgmol^{-1}$), this value was used directly. The density value of PCHPE was measured using PCHPE specimens prepared of similar molar mass (9.1 $kgmol^{-1}$) to the PCHPE blocks in the MBPE samples (ca. 9.0 – 11.4 $kgmol^{-1}$). The measurement was made using a solvent-cast PCHPE sheet which was carefully cut into regular-shaped specimens (5 mm × 5 mm × 0.2 mm). The exact dimensions, including width, length and thickness of each specimen, were measured and averaged at three different positions, using a calliper. The density was calculated as the average of three different samples, all of regular dimensions, giving a value of 1.04 ± 0.06 gcm^{-3}.

Shape-memory Effect. The shape-memory properties (fixed strain ε_f, residual strain ε_r, strain recovery capability, etc.) are defined or quantified using the following equations:

ε_f: the fixed strain after being stretched to ε_{max} = 300 % and left to relax freely at ambient temperature (18 °C).

$$\textbf{Strain fixity ratio} = \frac{\varepsilon_f}{\varepsilon_{max}} \times 100\% \quad (1)$$

ε_r: the remaining strain after being heated to 55 °C for 30 s and left to cool to ambient temperature (18 °C).

$$\textbf{Strain recovery ratio} = \frac{\varepsilon_{max} - \varepsilon_r}{\varepsilon_{max}} \times 100\% \quad (2)$$

Shape memory effect monitored by SAXS: preparation procedure of samples with a range of fixed strain. Sample bars were stretched to 300% and left to relax at ambient temperature (20 °C) to ca. 280% (fixed strain). Thereafter, stretched sample bars were placed on hot plate (55 °C) for predetermined time duration to reach different extent of recovery, followed by immediate liquid nitrogen quenching. Sample bars with a range of strain values (ca. 0%, 75%, 185% and 280%) were then submitted to SAXS characterization.

Investigation of polymer orientation in stretched MBPE-59 using 2D WAXS characterization

The 2D WAXS scattering pattern demonstrates an isotropic ring (Figure S17A), which could be indicative of weak polymer chain orientation. The 2D pattern was further analysed by selecting sectors with a width of 10° and integrating the intensity as a function of q. The 90° direction is perpendicular to the stretching direction. These sectors are plotted together in Figure S17B – there is no difference in intensity as a function of orientation which suggests either there is no orientation or it’s below the detection limit of 2D WAXS.

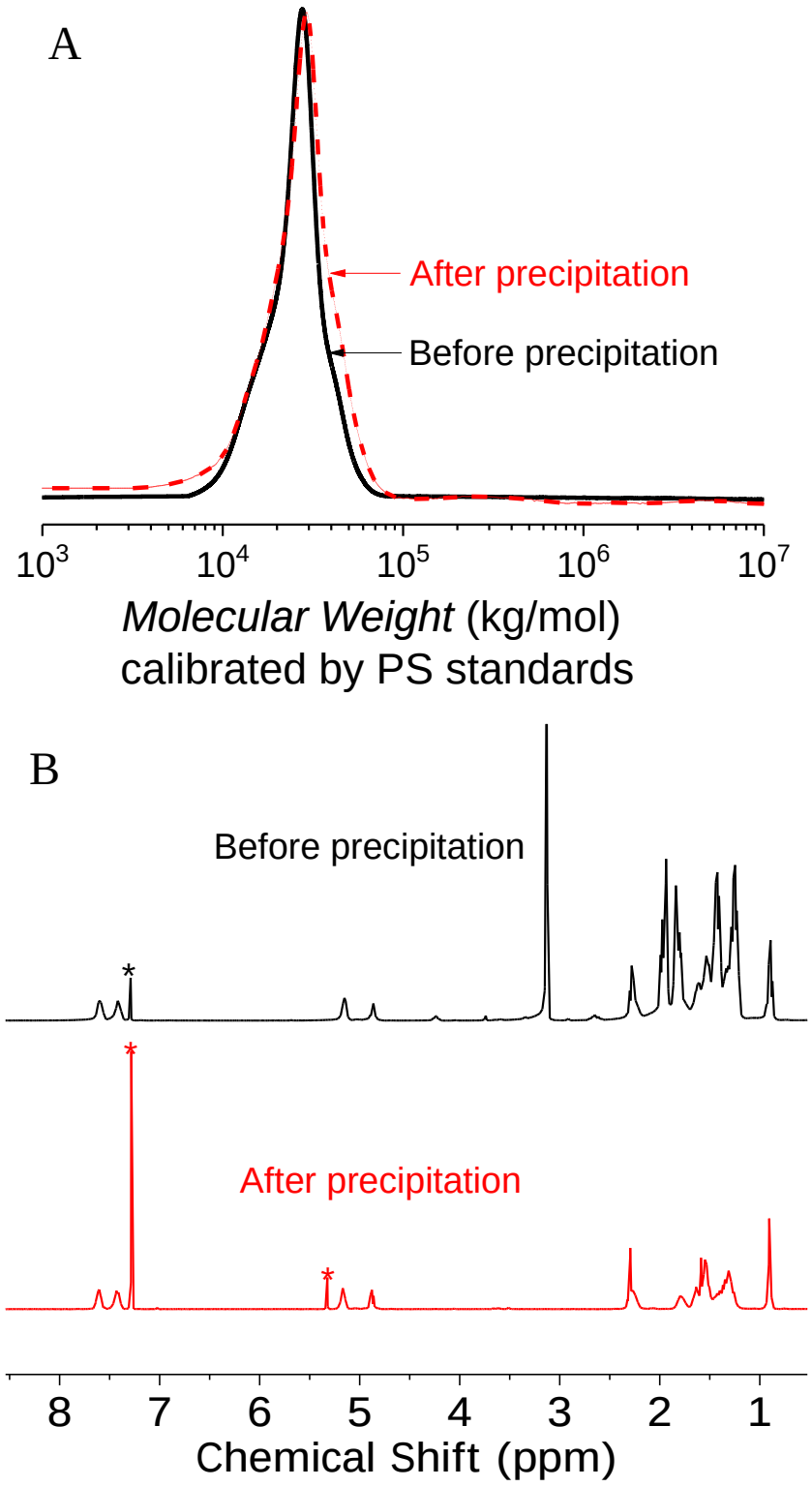

Figure S1. (A) The typical SEC traces and (B) ^{1}H NMR spectra of the triblock precursor to MBPE-42 (Table 1, #2), before (black curve) and after (red curve) precipitation using cold methanol.

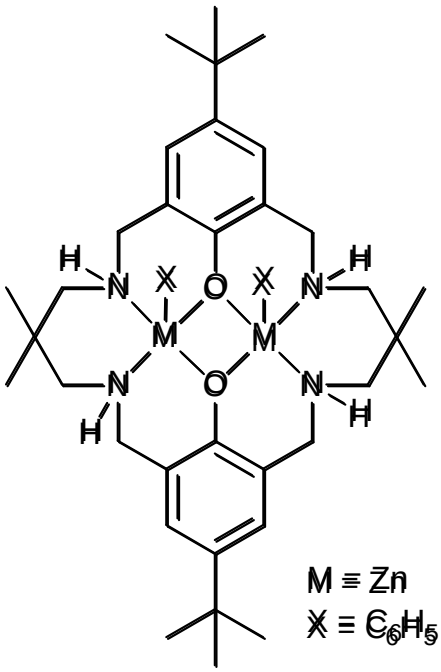

Figure S2. Chemical structure of $[LZn_2Ph_2]$.[1,2]

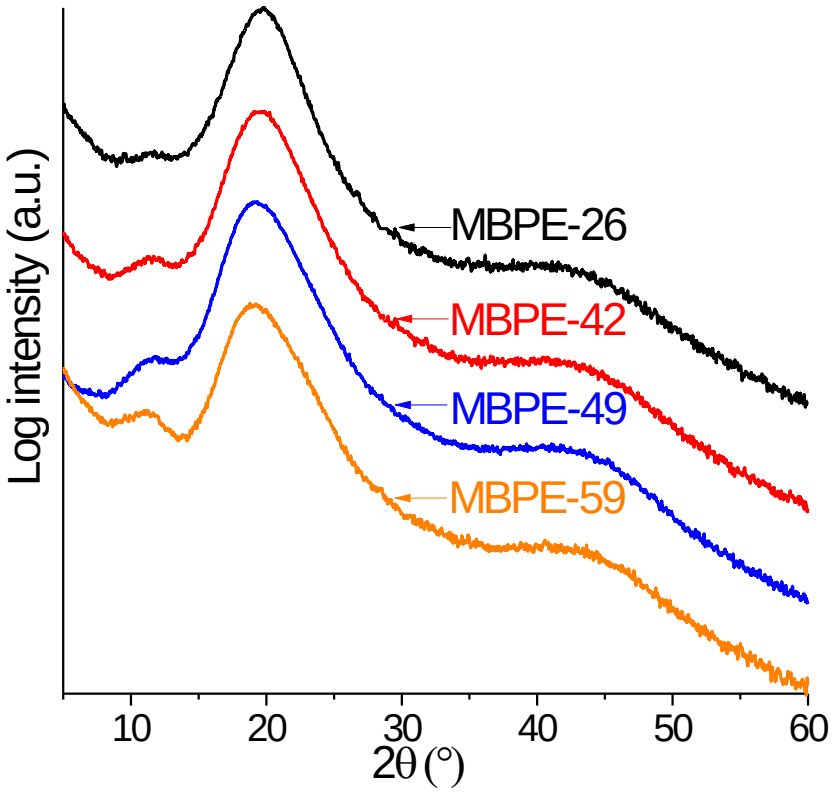

Figure S3. WAXS profiles of MBPEs (Table 1) after being thermally annealed at 130 °C for 48 h. The traces have been shifted vertically for clarity.

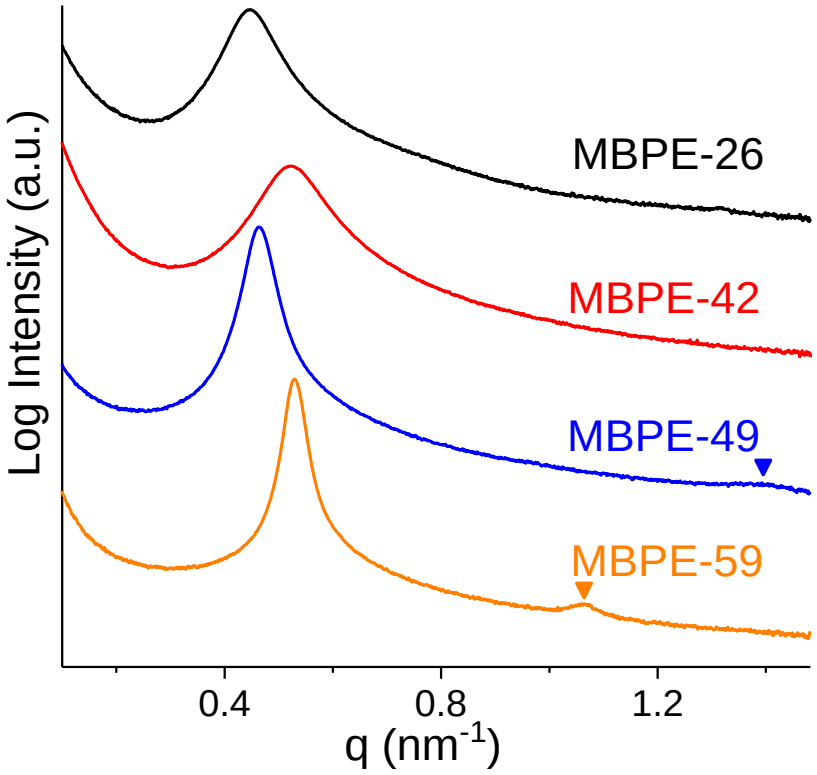

Figure S4. SAXS profiles of MBPEs (Table 1) after being thermally annealed at 130 °C for 48 h. Domain spacing (D) values are calculated (D = 2π/q) to be 14.1 nm, 12.1 nm, 13.5 nm and 11.9 nm, corresponding to MBPE-26, MBPE-42, MBPE-49 and MBPE-59, respectively. Secondary peaks can be observed in the MBPE-49 and MBPE-59 samples after annealing, indicating long range order. The traces have been shifted vertically for clarity.

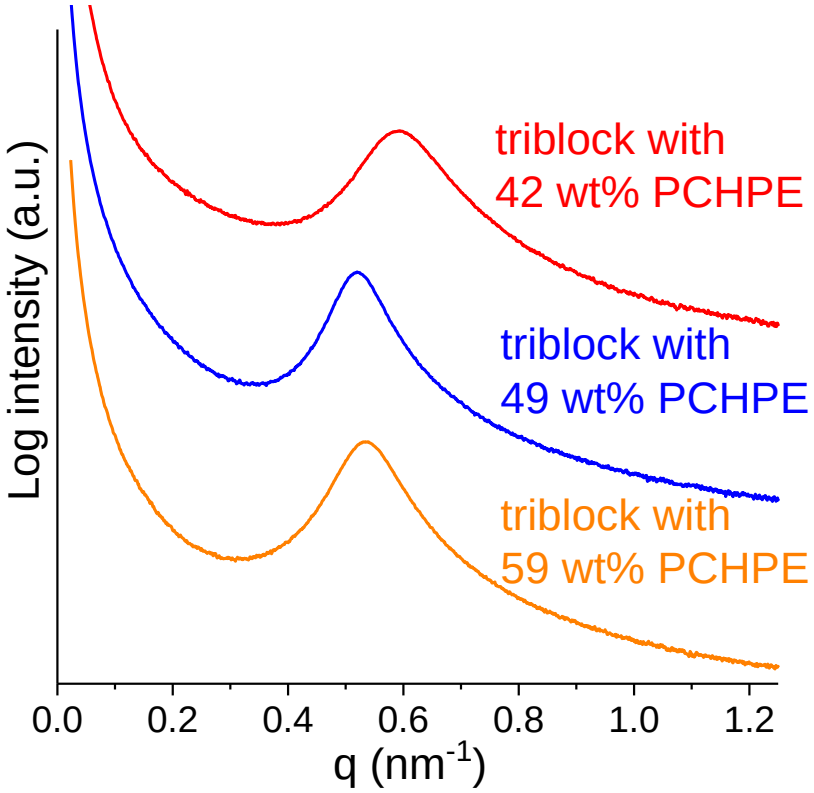

Figure S5. SAXS profiles of the triblock polyesters. Domain spacing (D) values are calculated ($D = 2\pi/q$) to be 10.6 nm, 12.1 nm and 11.8 nm, corresponding to 42 wt% PCHPE, 49 wt% PCHPE and 59 wt% PCHPE, respectively. The triblock polyester with 26 wt% PCHPE was not recorded as it was a viscous liquid which could not retain its shape outside of the mould. The traces have been shifted vertically for clarity.

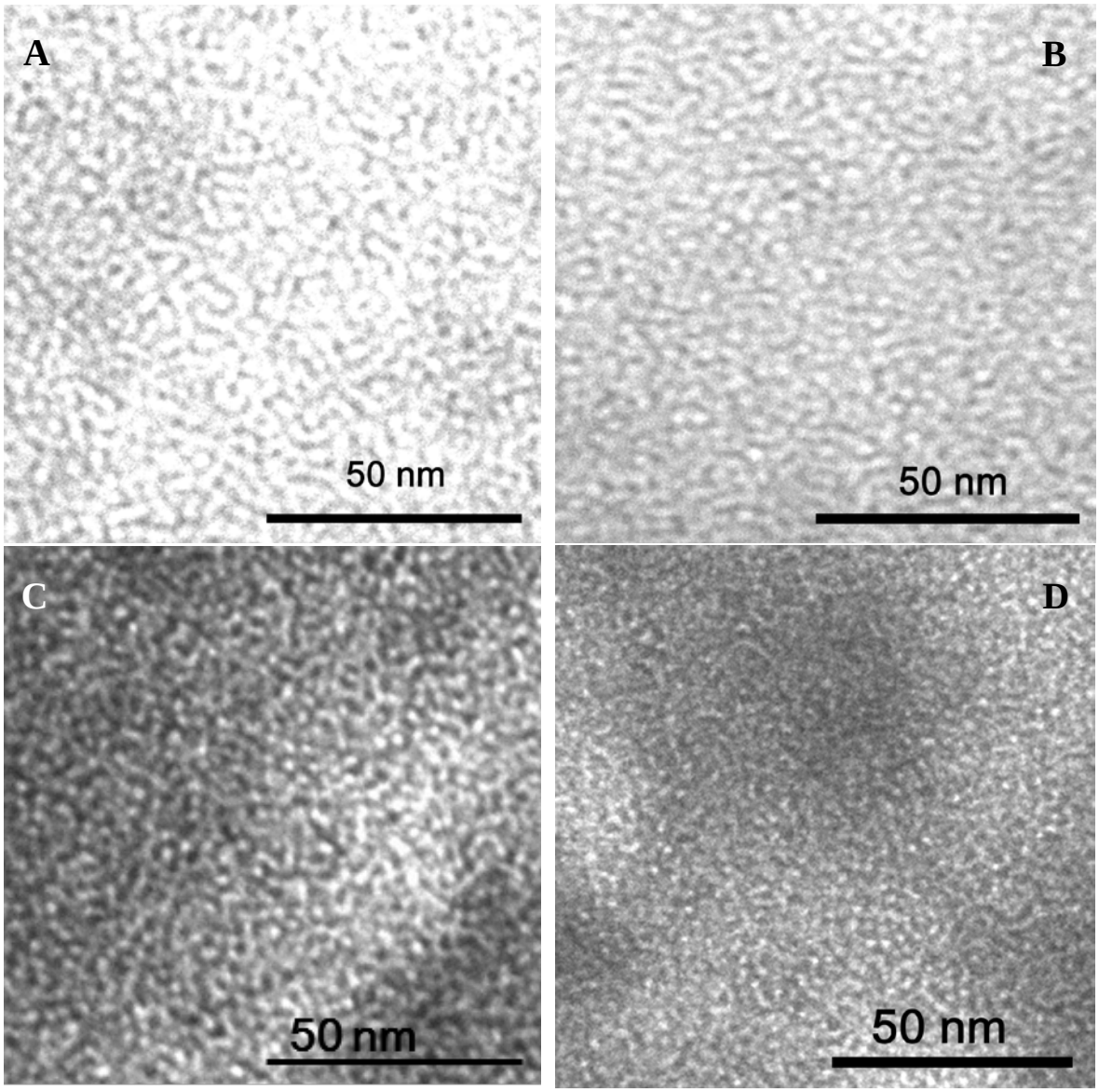

Figure S6. TEM images of MBPE samples (Table 1), stained with RuO_4 (which darkens the PCHPE domains) and sectioned by ultra-microtome. (A) MBPE-26; (B) MBPE-42; (C) MBPE-49; (D) MBPE-59.

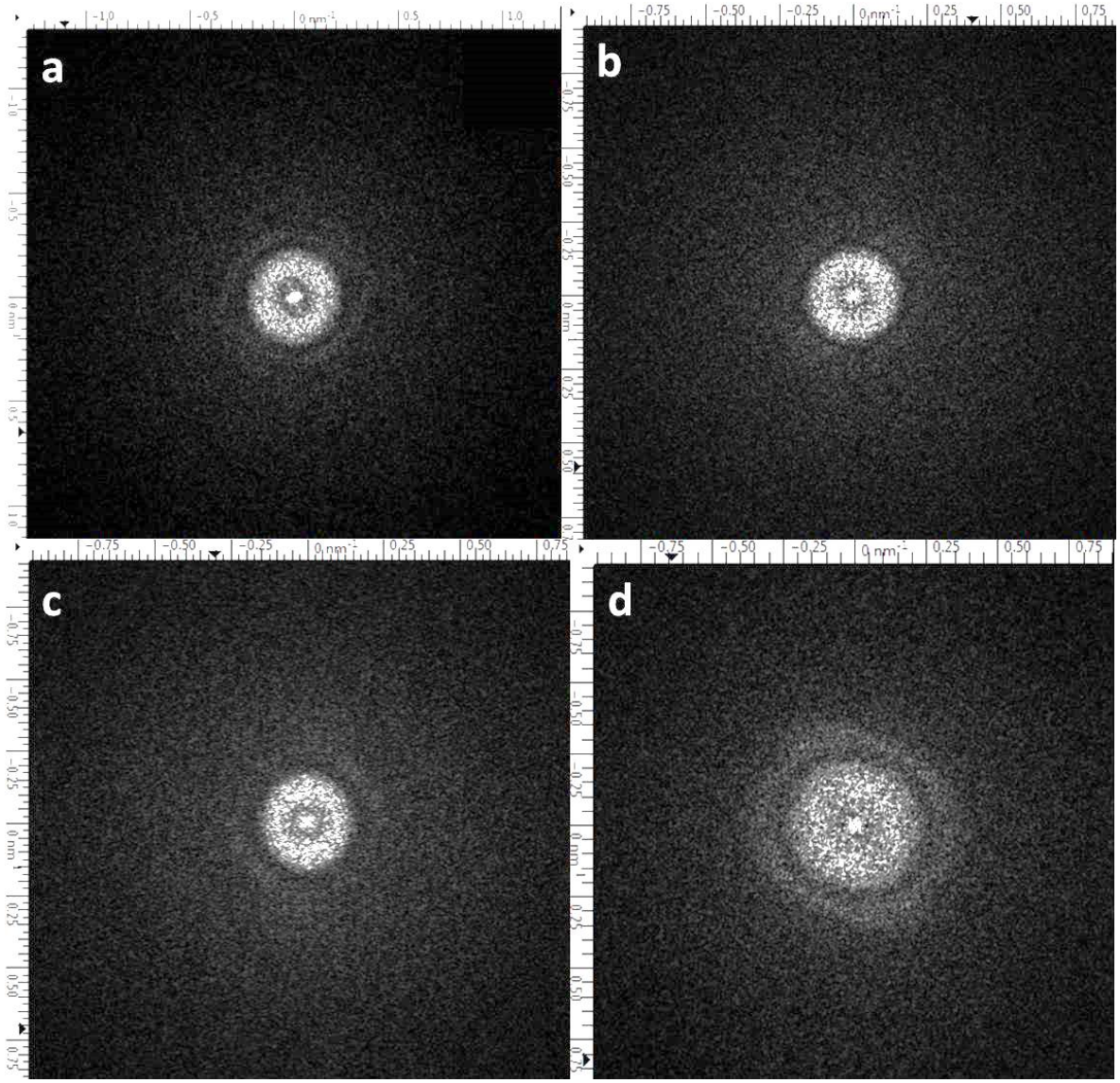

Figure S7. Frequency domain images acquired from TEM images shown in Figure S6 using the fast Fourier transform (FFT), a-d correspond to MBPE-26, MBPE-42, MBPE-49 and MBPE-59, respectively.

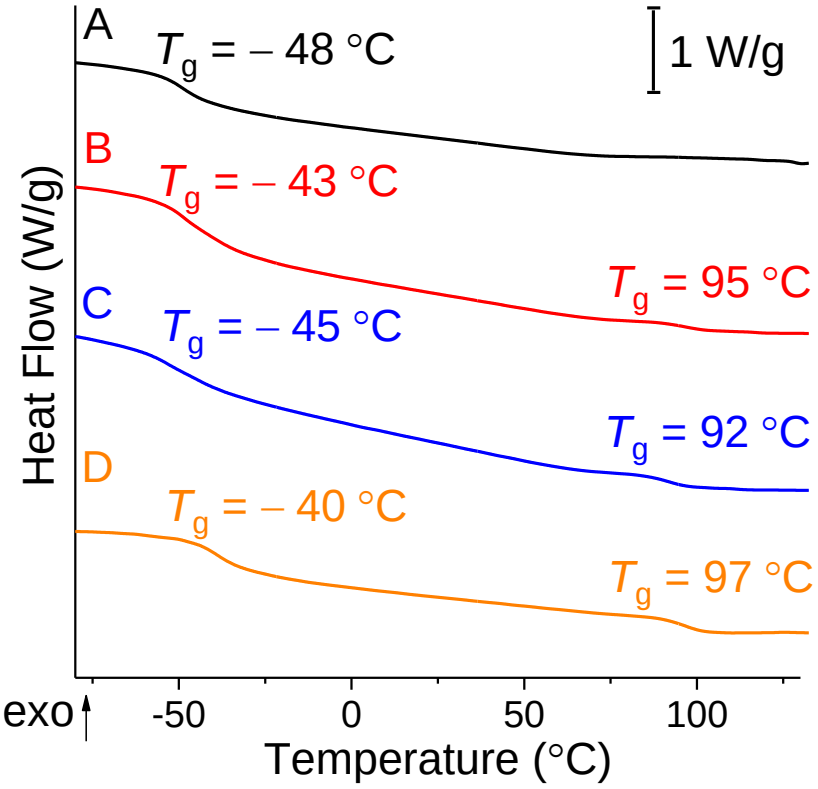

Figure S8. DSC thermograms of the triblock precursors: (A) 26 wt% PCHPE, (B) 42 wt% PCHPE, (C) 49 wt% PCHPE and (D) 59 wt% PCHPE (Table 1). The traces have been shifted vertically for clarity.

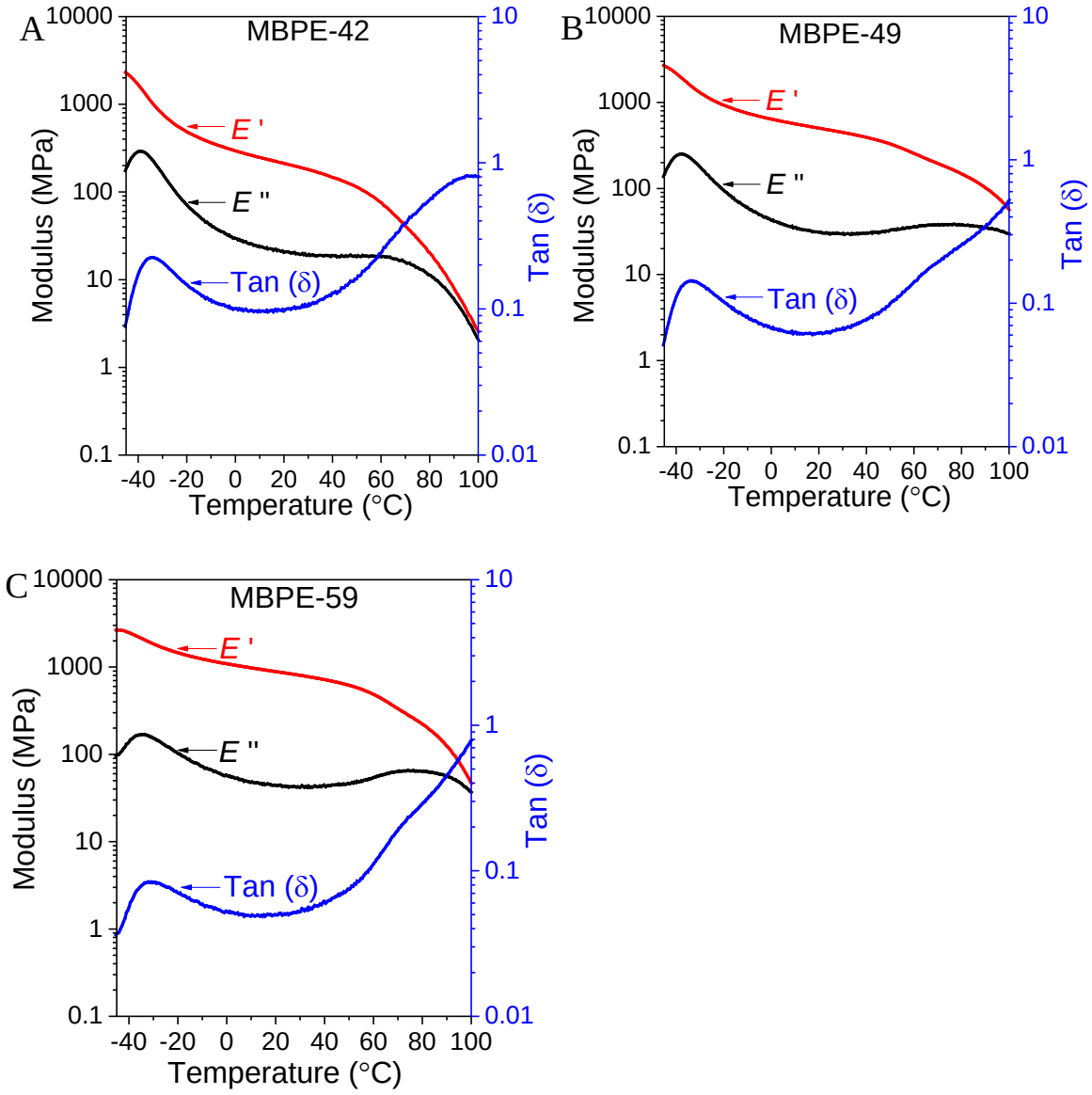

Figure S9. MPBE DMTA data showing the overlay of the storage modulus E', loss modulus E" and tan(δ). (A) MBPE-42, (B) MBPE-49, (C) MBPE-59. The DMTA conditions: ω = 1 Hz, strain = 1%, temperature ramp rate = 3 °C/min.

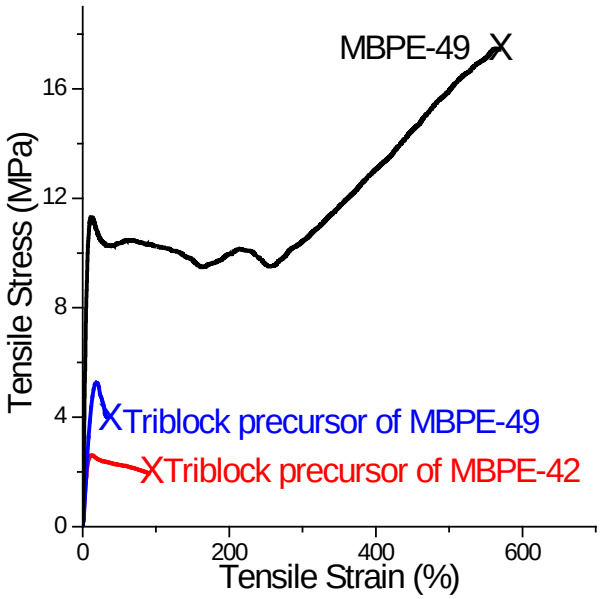

Figure S10. Representative stress-strain curves for uniaxial extension of the triblock precursors of MBPE-42 and MBPE-49. The stress-strain curve of MBPE-49 is also included for comparison. The failure points are marked with an 'X'. The tensile tests on the BAB precursors of MBPE-26 and MBPE-59 were not performed due to the difficulties in preparing sample bars. The BAB precursor to MBPE-26 is a soft semi-solid which deformed during sample loading and the BAB precursor to MBPE-59 was brittle and fractured during cutting.

Table S1. Mechanical properties of the triblock precursors to MBPE-42 and MBPE-49.[a]

Sample	E_y[b] (MPa)	σ_b[c] (MPa)	ε_y[d] (%)	ε_b[e] (%)
Triblock precursor of MBPE-42	26 ± 4	2.0 ± 0.7	17 ± 4	91 ± 11
Triblock precursor of MBPE-49	46 ± 7	3.9 ± 1.5	12 ± 6	33 ± 12

[a)] 95% confidence interval where the number of specimens is 3 in each case; [b)] Young's modulus; [c)] stress at break; [d)] strain at yield; [e)] elongation at break.

Strain-induced plastic-to-rubber transition

A strain-induced plastic to rubber transition was observed for MBPE-49. Firstly, the sample was extended to 350% strain, at the rate of 10 mm/min, and allowed to retract, at the same rate, until reaching 0 MPa stress. The sample was allowed to freely relax, at ambient temperature, for 1 h but did not fully regain its original shape. Indeed, a stretched sample did not fully retract even after being allowed to relax for an extended period (>1 year). After the sample was allowed to relax for 1 h, a second stress-strain cycle was applied to same overall strain (350%). The second and all subsequent stress-strain cycles show only elastomeric behaviour without any observable yield point. The unusual behaviour of this sample could be due to a change in microstructure during the first stress-strain cycle. It is proposed that during the first stress-strain cycle, the PCHPE continuous phase is disrupted to generate a new structure featuring isolated domains of PCHPE in a continuous matrix of PDL. This new morphology delivers the elastomeric behaviour observed in subsequent stress-strain cycles (Figure S11). A similar mechanical performance was observed for other block copolymers including poly(styrene-butadiene-styrene) and poly(styrene-*b*-butadiene-*b*-4-vinylpyridine and was also attributed to a strain-induced plastic-to-rubber transition.[4,5]

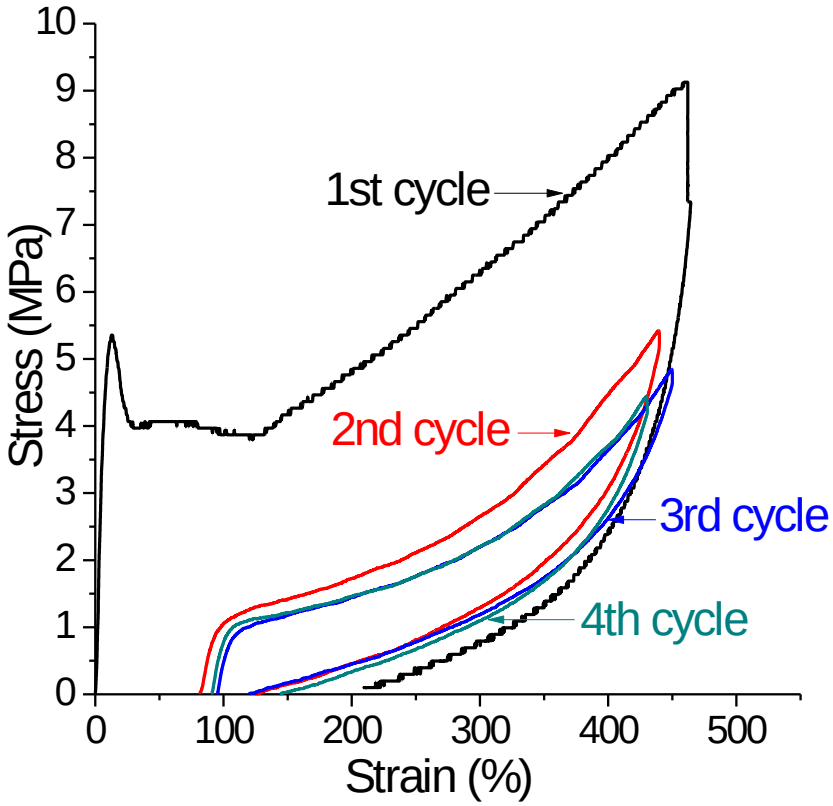

Figure S11. Strain stress cycle observed using MBPE-42 (Table S4 shows the complete hysteresis data). The sample bar was allowed to freely relax, at ambient temperature, for 1 h, between each cycle.

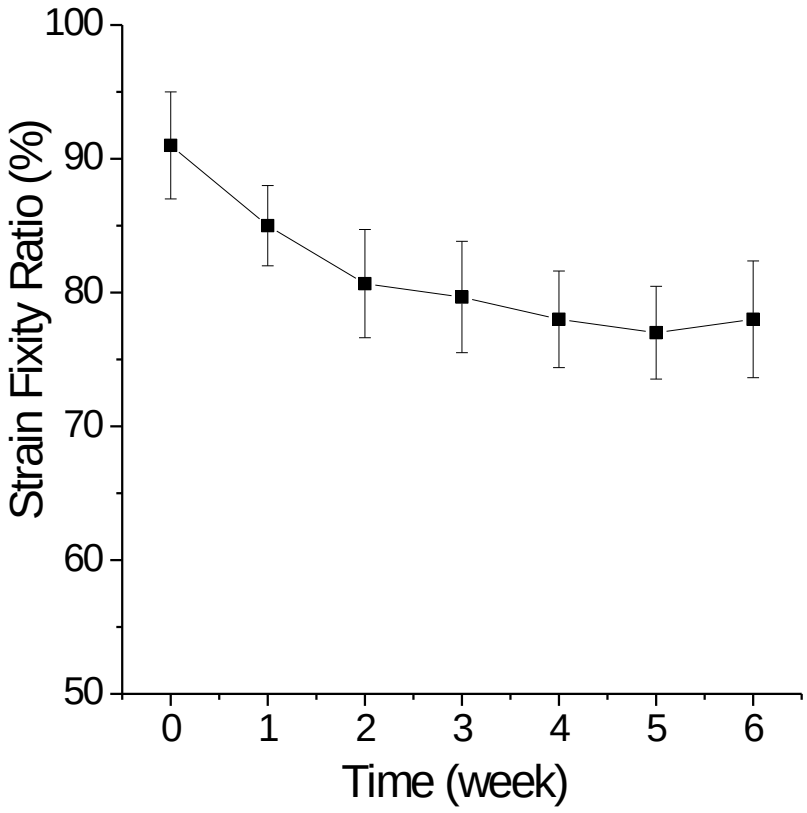

Figure S12. Relaxation of the pre-stretched MBPE-59 over 6 weeks. Although a slight decrease in strain fixity ratio was observed over the first week, there was no further decrease over the subsequent five weeks, confirming the requirement to heat the sample above the transition temperature (50 °C) to re-gain the original shape.

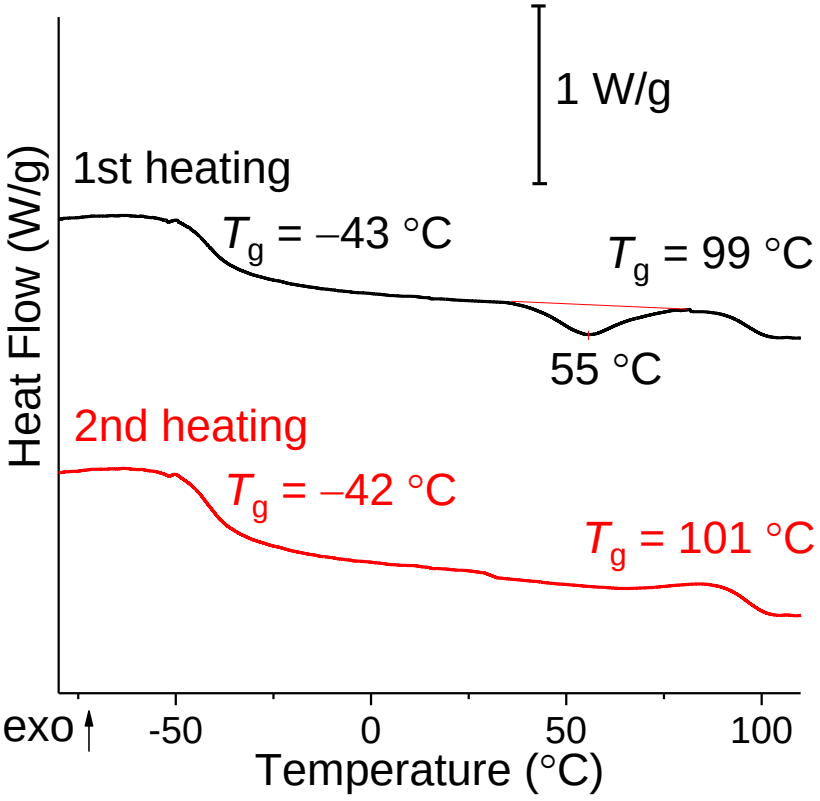

Figure S13. DSC thermogram (exothermic up) of stretched MBPE-59. T_g values are reported at the midpoint of each transition. The traces have been shifted vertically for clarity.

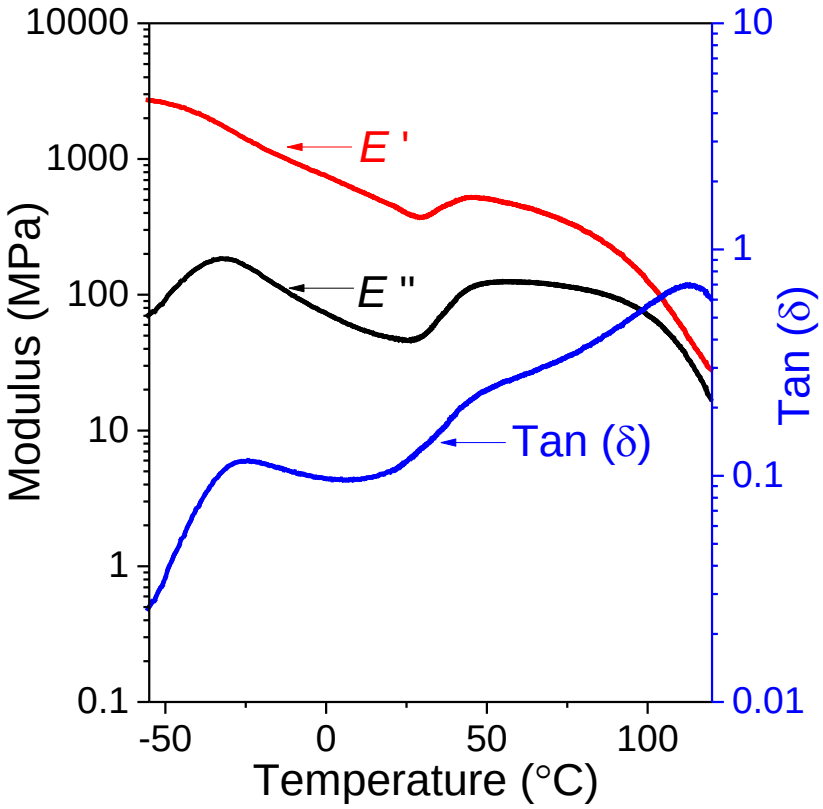

Figure S14. Overlay of the storage modulus, E', loss modulus, E", and tan(δ) of the stretched MBPE-59; conditions: ω = 1 Hz, strain = 1%, temperature ramp rate = 3 °C/min.

Mechanical performance of a mixture of MBPE-59 and 59 wt% triblock polyester (1/1, w/w)

To validate the supposition that residual triblock in significant concentration would compromise mechanical performance, the mechanical performances of MBPE-59 was compared with the mixture.

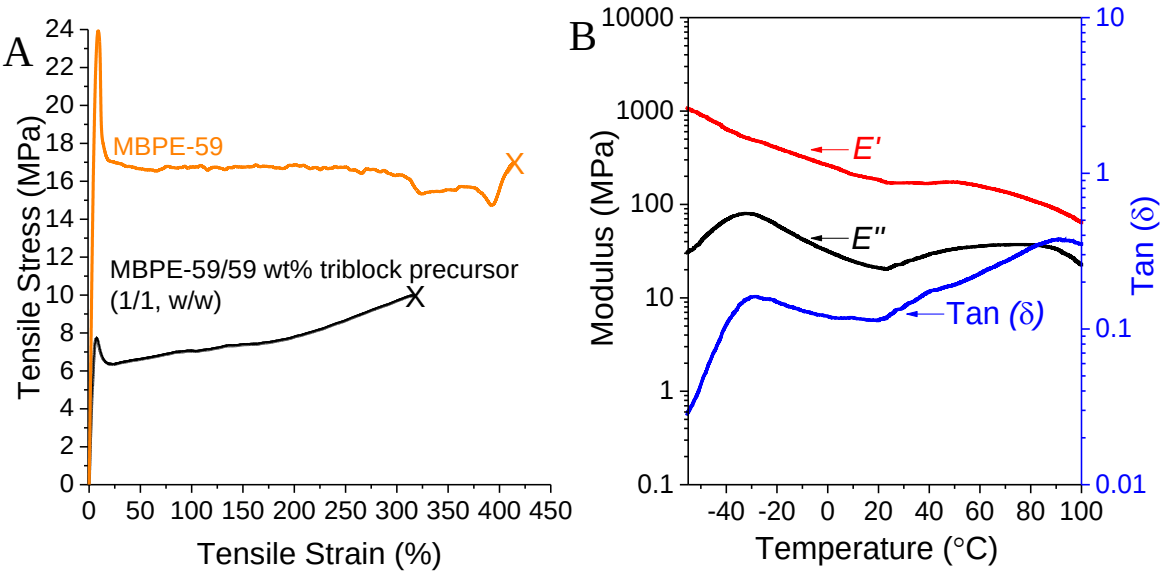

Figure S15. (A) The stress-strain data for uniaxial extension of the mixture of MBPE-59/59 wt% triblock precursor (1/1, w/w) compared with MBPE-59; (B) Overlay of the storage modulus, E', loss modulus, E'' and tan(δ) of the stretched mixture (i.e. MBPE_59:59 wt% triblock, 1:1); conditions: ω = 1 Hz, strain = 1%, temperature ramp rate = 3 °C/min.

Overall, the mixture shows worse mechanical data than MBPE-59, with a significantly lower Young's modulus (140 ± 5 MPa), strength at break (10 ± 2 MPa), and ε_b (310 ± 30 %). This compromise of mechanical performance indicates that any residual triblock in the MPBEs likely softens the materials. Additionally, DMTA analysis of the mixture sample which had been stretched showed a storage modulus peak at ~50 °C, indicating that the transition is unaffected by the residual triblock.

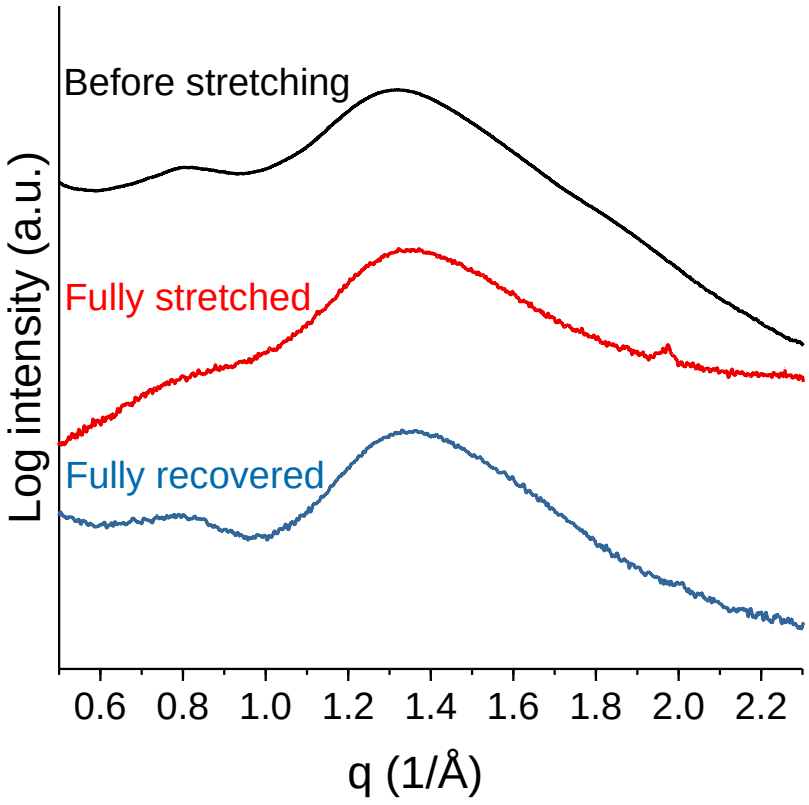

Figure S16. 1D WAXS profiles of MBPE-59 during a stretching and recovery cycle. The traces have been shifted vertically for clarity.

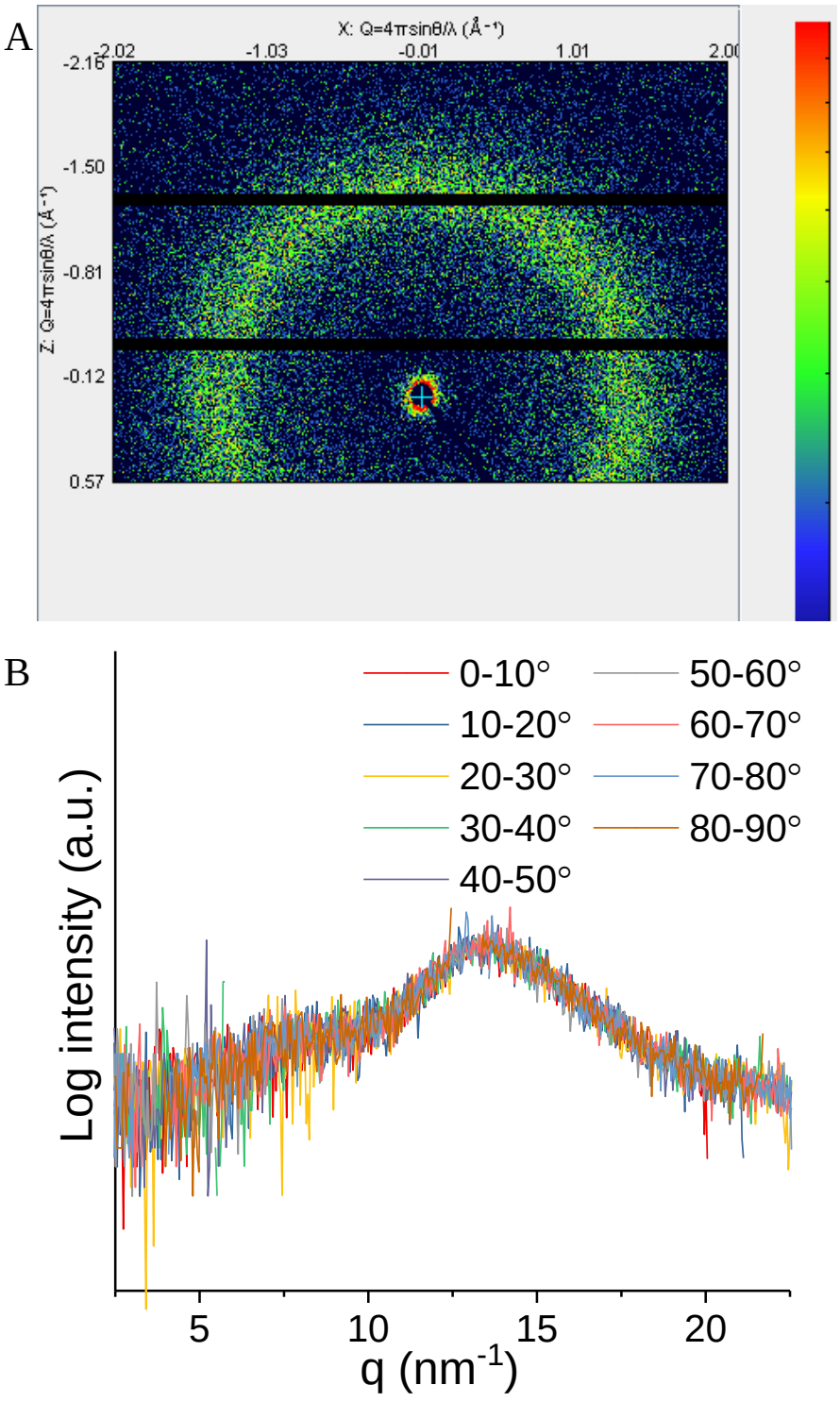

Figure S17. (A) 2D WAXS profile of the stretched MBPE-59; (B) Overlay of scattered intensity in the sectors between 0 and 90° as a function of q, corresponding to (A). Horizontal plane (0°) is the stretching direction. These samples were characterized at ambient temperature.

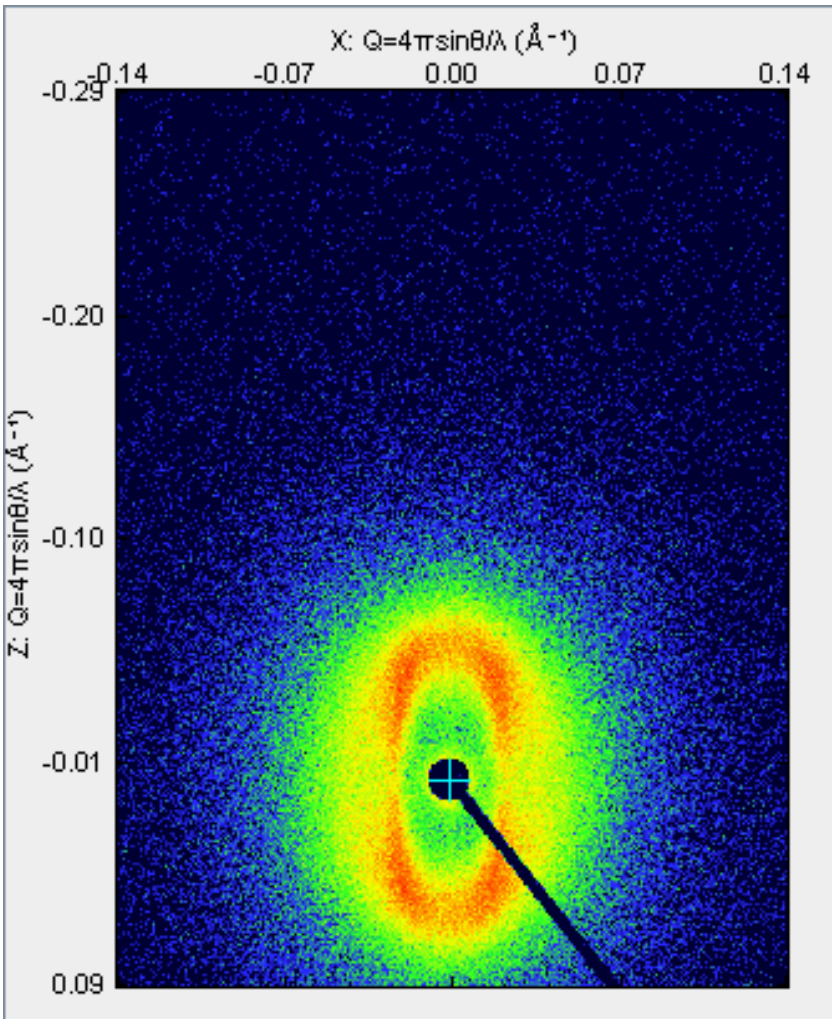

Figure S18. 2D SAXS profile of stretched MBPE-59. Horizontal plane is the stretching direction. These samples were characterized at ambient temperature.

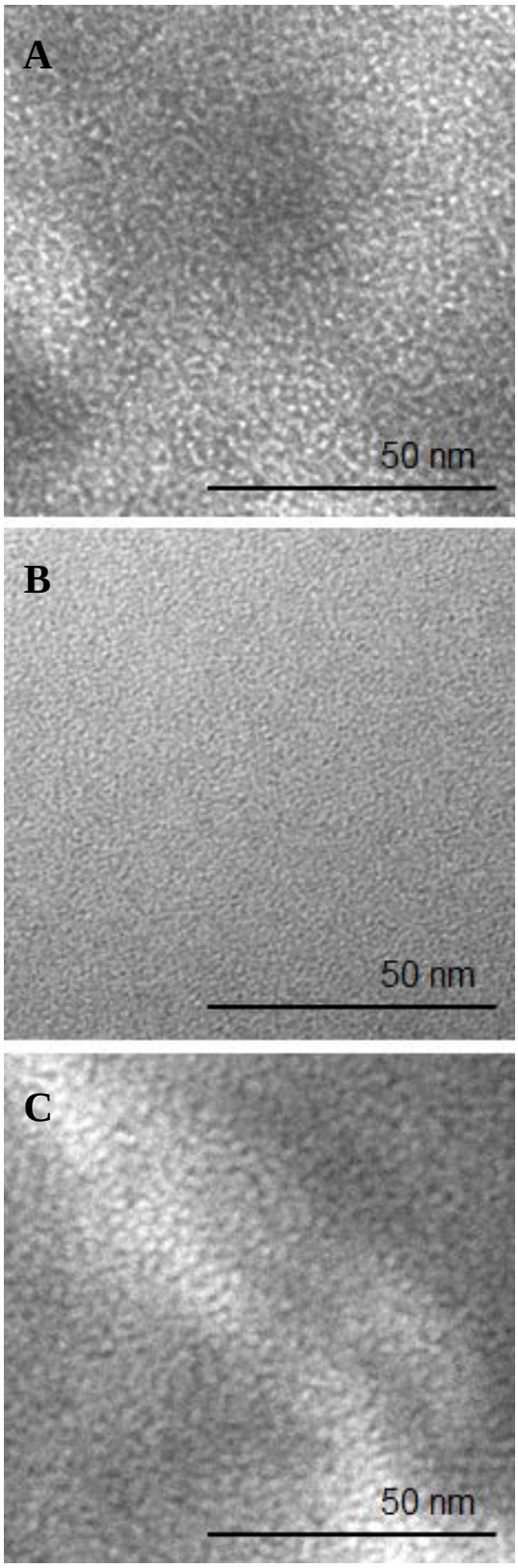

Figure S19. Cross-sectional (vertical to the extension direction) TEM images MBPE-59, evaluated as it was stretched (sectioned by ultra-microtome and stained with RuO_4). (A) Before stretching; (B) fully stretched; (C) fully recovered.

Table S2. Data of representative TPEs comprising block copolymers from both commercialized products and literature examples.

#	Polymer	Block architecture		σ_b (MPa)	ε_b (%)	Block composition	Resilience (%)	References
		Hard	Soft					
1	Hytrel (Dupont)	semi-crystalline poly(butylene terephthalate)	amorphous long-chain polyether glycols	10-31	200-375	N.A.	N.A.	([6])
2	Skypel (SK chemicals)	semi-crystalline polymer	amorphous polymer	22-50	350-900	N.A.	47-72 (ASTM D2632)	([6])
3	Riteflex (Celanese)	N.A.	N.A.	20-31	50-350	N.A.	N.A.	([6])
4	Pibiflex (SO.F.TER)	semi-crystalline poly(butylene terephthalate)	amorphous long-chain polyether	11-40	400-900	N.A.	N.A.	([6])
5	Kopel (Kolon)	semi-crystalline poly(butylene terephthalate)	amorphous polyether	25-39	400-850	N.A.	N.A.	([6])
6	RTP 1500 series (RTP)	N.A.	N.A.	8-40	200-550	N.A.	N.A.	([6])
7	PEBAX (Arkema)	semi-crystalline polyamide	amorphous polyether	34-63	300-640	N.A.	N.A.	([6])
8	Styron Sprintan (SBS)	semi-crystalline polystyrene	amorphous polybutadiene	19-22	380-520	21-40% polystyrene	18-27 (ISO-4662)	([6])
9	P(L)LA–PβMδVL–P(L)LA	semi-crystalline poly-(L)-lactide	amorphous poly(β-methyl-δ-valerolactone)	2-28	190-1790	32-54 wt% poly-(L)-lactide	N.A.	([7])

10	PS-PSB(M)A-PS	semi-crystalline polystyrene	amorphous soybean oil derived polymer	~1-12	~30-190	25-50 wt% polystyrene	N.A.	([8])
11	PAMMS-PMYR-PAMMS	poly(α-methyl-*p*-methylstyrene)	polymycene	0.5-9.9	525-1340	12-29 wt% poly(α-methyl-*p*-methylstyrene)	N.A.	([9])

Table S3. Hysteresis data of MBPE-26 after cycles.[a]

cycles	Residual strain (%)	loss ($J \cdot m^{-3} \cdot 10^4$)	Hysteresis (%)
1	3.7	23	21.6
2	2.8	14	12.5
3	4.1	11	11.8
4	5.1	13	14.3
5	4.2	13	15.1
6	3.1	12	14.1

[a)]*Data were calculated from cyclic loading—unloading (hysteresis) study on the MBPE-26 (6 cycles from 0% to ~200% strain at the velocity of 10 mm/min), corresponding to Figure 3B.*

Table S4. Hysteresis data of MBPE-42 after cycles.[a]

cycles	loss ($J \cdot m^{-3} \cdot 10^4$)	Hysteresis (%)
1	2200	83
2	450	50
3	330	43
4	350	50

a) *Data were calculated from cyclic loading—unloading (hysteresis) study on the MBPE-42 (velocity of 10 mm/min), corresponding to Figure S11.*

References

(1) Zhu, Y.; Romain, C.; Williams, C. K. *J. Am. Chem. Soc.* **2015**, *137*, 12179–12182.
(2) Romain, C.; Garden, J. A.; Trott, G.; Buchard, A.; White, A. J. P.; Williams, C. K. *Chemistry – A European Journal* **2017**, *23*, 7367-7376.
(3) Martello, M. T.; Schneiderman, D. K.; Hillmyer, M. A. *ACS Sustain. Chem. Eng.* **2014**, *2*, 2519–2526.
(4) Hashimoto, T.; Fujimura, M.; Saijo, K.; Kawai, H.; Diamant, J.; Shen, M. In *Multiphase Polymers*; American Chemical Society: 1979; Vol. 176, p 257–275.
(5) Arai, K.; Kotaka, T.; Kitano, Y.; Yoshimura, K. *Macromolecules* **1980**, *13*, 1670-1678.
(6) Fakirov, S. *Handbook of Condensation Thermoplastic Elastomers*; WILEY-VCH Verlag GmbH & Co. KGaA: Weinheim, 2005.
(7) Xiong, M. Y.; Schneiderman, D. K.; Bates, F. S.; Hillmyer, M. A.; Zhang, K. C. *PNAS* **2014**, *111*, 8357–8362.
(8) Wang, Z.; Yuan, L.; Trenor, N. M.; Vlaminck, L.; Billiet, S.; Sarkar, A.; Du Prez, F. E.; Stefik, M.; Tang, C. *Green Chem.* **2015**, *17*, 3806–3818.
(9) Bolton, J. M.; Hillmyer, M. A.; Hoye, T. R. *ACS Macro Lett.* **2014**, *3*, 717–720.